

Al and Zn Foams Blown by an Intrinsic Gas Source

By *M. Mukherjee,* F. Garcia-Moreno, C. Jiménez, J. Banhart*

[*] *Dr. M. Mukherjee, Dr. F. Garcia-Moreno, Dr. C. Jiménez, Prof. Dr. J. Banhart
Helmholtz-Zentrum Berlin
Hahn-Meitner-Platz
14109 Berlin, Germany
and
Technische Universität Berlin
Hardenbergstrasse 36,
10623 Berlin, Germany
E-mail: manas.mukherjee@gmail.com*

Abstract

A method was developed to produce Al- and Zn-based foams with a uniform distribution of small cells. Pre-alloyed AlMg50 powder containing hydrogen was used as a replacement for the usual blowing agent TiH₂. AlMg50 powder released gas uniformly in the entire sample, caused the nucleation of a large number of cells and led to simultaneous growth that finally resulted in a uniform cell structure. The expansion behaviour of these foams was studied by means of in-situ X-ray radiography. The macrostructure of the solidified foams was then analysed through optical microscopy and X-ray tomography and proved to be very uniform. The high strength of the foams was demonstrated by uni-axial compression tests.

1. Introduction

Although metal foams have some good weight-specific properties the scatter in cell size and shape as well as the presence of cell wall imperfections etc. have an adverse effect on their performance.^[1,2] Up to now, no experimental proof exists that metal foams with a structure that is considered “good”, i.e. having a uniform cell size distribution and smoothly curved cell walls, have better mechanical properties than irregular foams (not speaking of

deliberately graded foams). Still, there is good reason to believe that more uniform structures will facilitate application simply because their properties are easier to predict. In the same sense, smaller cells are desirable since a given foam volume will then contain more cells which leads to a better averaging of properties.^[3] Many irregularities in metal foams are believed to have their origin in the process of cell generation.^[4] A failure to create cells of uniform size in an early stage will be exacerbated during the ensuing coarsening process during growth of the foams.

The Ti or Zr hydrides usually used for blowing foams are extremely effective gas sources that liberate large amounts of hydrogen in the melting range of Al- and Zn-based alloys. Provided that these hydrides are pre-treated appropriately, damage of the emerging foam by premature gas release can be limited.^[5] Still, hydrogen production by TiH_2 or ZrH_2 extends over a large temperature and time interval, which was identified as a possible source for the generation of irregular pores.^[6,7] To overcome this effect, a method was developed that leads to a more gentle and less localised gas production in a liquid metal by using physically and chemically adsorbed gas in constituents of the alloy itself. AlMg50 pre-alloyed powder (containing 50 wt.% of each element) was found to be such an intrinsic gas source.^[8] Magnesium (beside silicon and copper) is an important alloying element and was found to lead to Al foams with good expansion properties.^[9]

We show that very uniform foams can be produced using pre-alloyed AlMg50 powder and that the mechanical properties of such foams are very promising.

2. Experimental

2.1. Materials

Aluminium (Alpoco, 99.7% pure), copper (Chempur, 99.5% pure) and zinc (Grillo Werke, 99.99% pure) metal powders and pre-alloyed AlMg50 powder (Possehl Erzkontor GmbH, purity not known) were used to prepare foamable precursors (all in wt.%). No

additional conventional blowing agent, e.g. hydride or carbonate, was used. Pre-alloyed AlMg50 powder contains significant amounts of hydrogen^[10] and was therefore used both as intrinsic gas source and as alloying element. The four alloys investigated in the present study are specified in Table 1. When blending the powders, the amount of AlMg50 was adjusted to achieve the desired weight fraction of Mg in the alloy. All powders were mixed in a tumbling mixer for 15 min. The powder blend was subjected to uni-axial hot compaction applying 300 MPa pressure for 15 min. The compaction temperature for each alloy is given in **Table 1**. Cylindrical tablets (36 mm diameter, ~11 mm thickness) were obtained. Small samples of dimensions 10×10×4 mm³ were cut out from these tablets, ensuring that the compaction direction (defining the foaming direction) was along the 4 mm long side of the sample. These small samples were used for studying the expansion behaviour by means of in-situ X-ray radioscopy. For compression tests and three-dimensional (3D) pore size analysis, samples were produced by melting and foaming an entire tablet.

2.2. Foaming procedure

All the foaming trials were performed under ambient atmosphere and pressure. Foaming was carried out by heating the precursors on top of a ceramic heating plate that can be powered up to 600 W. The sample temperature was measured by a thermocouple led through the heating plate that was in contact with the lower surface of the foaming sample. As this thermocouple is influenced by the heating plate, the measured temperature deviates from the true interior sample temperature. This required additional calibration experiments using two thermocouples – one at the bottom surface and another inside the sample. It was observed that during the isothermal holding stage, i.e. after reaching the maximum foaming temperature, the surface temperature was about 10–15 °C above the true interior temperature. The temperatures given in the following refer to the surface temperature.

Foaming was continuously monitored *in-situ* by using a X-ray radioscopy set-up comprising a micro-focus X-ray source and a panel detector as described in Ref.^[13]. In this work, the X-ray spot size was set to 5 μm applying 100 kV voltage and 100 μA current. Series of X-ray-projected images of the foaming samples were obtained and analysed with the dedicated software AXIM^[14]. Expansion is measured in terms of the growth of the projected area of the sample. True volume expansion will be higher. However this cannot be estimated for the entire foaming period since AXIM calculates the volume of the sample assuming that its cross section parallel to the X-ray beam is circular. Therefore this volume data is correct only after the precursor has melted completely and surface tension has made the cross sections circular.

2.3. Structural and mechanical characterization

Compression tests and 3D pore size analysis were performed for the AlMg15Cu10 alloy. X-ray tomography was performed using the same X-ray set-up used for radioscopy, but in addition rotating the samples through 360° in 1000 steps while acquiring images after each step. 3D reconstruction of the data was performed using the commercial software Octopus. The reconstructed data was analysed using the software MAVI 1.3.1.

Compression tests were carried out on four samples. The outer skins of all the foams were removed to prepare samples of average dimensions $27 \times 17 \text{ mm}^2$ in cross section and 14 mm in height ensuring that the height is along the compaction direction. Quasi-static compressions were carried out in a Materials Test System (MTS 810) at a displacement rate of 1 mm/min.

3. Results

3.1. Foam expansion

Although no conventional blowing agent was used, all the alloys foamed and reached moderate foam expansions. The expansion behaviour of the Al and Zn alloy foams is shown in **Figure 1**. In both alloys, expansion increases with increasing content of Mg (i.e. AlMg50 powder) and with increasing foaming temperature. For example, compare the expansion of AlMg26Cu10 foamed at 550 and 600 °C given in Figure 1a. Both Al-based foams are stable during isothermal holding as expressed by the near-plateau region of the expansion profile. ZnAl3.3Mg3.3 foams are stable for an even longer period, whereas ZnAl5.2Mg5.2 foams collapse almost immediately after reaching maximum expansion. It can be seen that Zn-based samples expand more than Al-based samples even though Zn-based samples contain less amounts of AlMg50 powder. As discussed earlier, i.e. assuming circular symmetry around foaming axis, the maximum volume expansions in the liquid state and after solidification were measured by AXIM and the values are given in Table 1.

The stability of the Al-based foams was not tested for longer isothermal holding since the high temperature needed to foam these alloys results in heavy oxidation of the Mg present in the alloy and leads to a burnt outer surface. Therefore, extended holding was avoided. Oxidation can be so severe that if AlMg26Cu10 foam is left for a longer period at 600 °C, the foam starts to burn with a red glow due to the highly exothermic oxidation of Mg.

3.2. Foam structure

Figure 2 shows representative 2D macrostructures of all the alloy foams studied. Al alloy foams contain larger cells (average 1.3–1.5 mm) compared to those in Zn alloy foams where the average cell diameter is about 0.6–0.8 mm. The AlMg15Cu10 alloy foams appear almost defect-free with smooth and uniformly curved cell walls, see Figure 2a. In the other alloy foams (Figures 2b–2d), some defects – elliptical cells and missing or broken cell walls – are visible. The cells in the AlMg26Cu10 are mostly polyhedral with thin cell walls suggesting a lower density than AlMg15Cu10 foams. Both small and large cells are present in

the micrograph shown in Figures 2c and 2d. On the other hand, in Al alloy foams the cell size distribution is very narrow as evidenced by both the 3D section shown in the inset of the **Figure 3** and the corresponding 3D cell size distribution. We find a uni-modal distribution and a peak at a cell diameter of 1.95 mm. The mean cell diameter is greater than that observed in the 2D micrograph of small samples in Figure 2a.

The density of the AlMg15Cu10 foams determined from the larger samples prepared for compression tests is about 0.72 g.cm^{-3} . The density of the AlMg15Cu10 precursors is 2.77 g.cm^{-3} . Hence, the relative density of the foams is about 26% implying a volume expansion of almost 285%. The calculated porosity (73.4%) in the 3D analysis is in agreement with the measured density. Note that the expansion of the Zn-based alloy foams is higher than that of Al-based alloy foams. This suggests a lower density for the Zn alloy foams, see Table 1. It is also noticeable that the density of the large foams is slightly lower than that of the small foams studied by radioscopy.

3.3. Compressive strength

The stress-strain response of AlMg15Cu10 foam as shown in **Figure 4** reveals a high plastic strength. The initial part is almost linear before the stress reaches a peak stress of 32 MPa, after which it falls to a value of about 14 MPa upon further straining and then fluctuates around a plateau stress of 18 MPa. This indicates a brittle nature of deformation. The average peak stress determined from the compression tests of four samples is $36 \pm 3 \text{ MPa}$.

4. Discussion

Hydrogenated Al-Mg alloys are known for their hydrogen storage capacity.^[15,16] In the present case, however, the AlMg50 powder has not been hydrogenated. When exposed to ambient atmosphere, Al-Mg alloys can react with the atmospheric moisture and at first adsorb hydrogen at the surface from where it eventually migrates to the grain boundaries where it is

absorbed and forms MgH_2 .^[17,18] This is known to cause hydrogen embrittlement in these alloys.^[19,20] The pre-alloyed AlMg50 powder used in the present study consists of a single intermetallic phase $\gamma\text{-Al}_{12}\text{Mg}_{17}$. Mass spectrometric analysis of this intermetallic powder has shown that it releases hydrogen from 330 °C, peaking at 423 °C.^[10] The intrinsic hydrogen content of AlMg50 powder is sufficient to achieve a moderate expansion both in Al- and Zn-based alloys, see Figure 1. In powder compact method, volume expansions of 350–650% for Al and Al-based alloys^[21–27] and 600–1000% for Zn and Zn-based alloys^[21,26,28,29] have been reported in the literature.

It is generally believed that a favourable foaming condition is when most (preferable all) of the metallic part melts before gas generation from the blowing agent in the sample begins^[5,25,30,31] provided that there are sufficient numbers of gas nuclei in the material^[9]. Among the alloys used in the present study, the Zn-based alloys fulfil this requirement quite well: the near eutectic Zn-alloy containing 3.3 wt.% Mg melts at 340 °C (see Table 1) which is almost at the onset (330 °C) of gas generation from AlMg50 powder and well below the gas evolution peak^[10]. The other Zn-alloy with 5.2 wt.% Mg starts melting at 340 °C and is fully molten at the gas evolution peak temperature. Hence, the hydrogen gas is efficiently used when foaming these Zn-alloys. In contrast, the Al-based alloys start melting above the gas evolution peak temperature, see Table 1. This indicates that some part of the hydrogen gas is lost through residual porosity when foaming Al-based alloys. This may contribute to the lower expansions of the Al alloys compared to the Zn alloys. This is also observed for Al and Zn foams blown with TiH_2 .^[21]

The density of the foams produced from small samples (used for radioscopy) is higher than that of larger samples used to make test specimens. Since small samples have a higher specific surface area, gas loss during foaming of such samples is always greater. Consequently, the expansion of the small samples is lower. Since cell size and density are approximately inversely related,^[32] the average cell size in the small samples is lower.

Compared to the use of TiH_2 (typically 0.5 wt.%) there are more gas-releasing centres in the precursor containing AlMg50 powder since each particle acts as gas source there. Moreover, the gas source is an area source for AlMg50 instead of a point source as for TiH_2 as visualised in **Figure 5**. During decomposition, the hydrogen gas pressure is more evenly distributed in the foam blown with AlMg50. TiH_2 is an isolated source and the gas flux is expected to be high along the grain boundaries due to the large hydrogen concentration gradient. In contrast, when using AlMg50 these gradients are small and the gas sources are evenly distributed in the sample. As a result of these factors, the foam develops a large number of small and more uniformly sized cells, see Figures 2 and 3.

The solidified foam structures exhibit a low number of defects. This is due to the simple gas evolution characteristics (only one peak) of AlMg50 powder. The release of gas is completed in a short time and therefore the foam becomes stable as shown by the expansion of ZnAl3.3Mg3.3 in Figure 1b. Conventional blowing agents such as TiH_2 release hydrogen over an extended period and even up to high temperatures^[5,30,31,33] and also in a more localised way. Moreover, hydride particles of different sizes have different gas release characteristics. This leads to large pressure gradients in the foam and to instabilities causing cell wall rupture.^[32] When rupture occurs due to strong hydrogen release during solidification, defects are created.^[6,7]

Although ZnAl5.2Mg5.2 expands more than the Al alloys, the foams start to collapse shortly after reaching maximum expansion, see Figure 1b. This is a typical behaviour of foams produced from Zn and Zn-based alloys.^[28,29] The collapse could be because of (a) less pronounced stability in the Zn system due to a lower oxide content of the Zn powders,^[29] and (b) a too high temperature at which the foam structure is weak because of a low viscosity of the melt^[26] and therefore collapses due to its own weight (hydrostatic pressure) which is higher for Zn than for Al. The collapse is further accelerated by gravity-driven drainage.

The peak stress of AlMg15Cu10 as given in Figure 4 is higher compared to Al-foams of a similar density but blown with TiH₂. For instance, the peak strength of Al alloy foams with similar density is usually 15–20 MPa.^[21,23,34,35] The high strength of AlMg15Cu10 foams can be attributed to two factors. Firstly, the uniform cell size distribution, the lower average cell size and low number of defects. Secondly, the presence of intermetallic phases in the metallic matrix. According to the phase diagram of Al-Cu-Mg, the microstructure contains primary Al and intermetallic phases Al₆CuMg₄ and Al₈Mg₅.^[11] The presence of high amounts of intermetallic phases not only strengthens the matrix but also makes the foam brittle.

5. Summary and outlook

Foaming of Al- and Zn-based alloys was performed by the powder compact route but without using a conventional blowing agent. It was demonstrated that that using pre-alloyed AlMg50 powder as a constituent of the powder mixture, Al and Zn-based alloys can be foamed under atmospheric pressure. The hydrogen content in AlMg50 powder was found sufficient for foaming and acts as an intrinsic gas source. The resulting foams show a uniform distribution of ≈ 0.7 mm (Zn-based) or ≈ 1.95 mm-sized cells (Al-based). Due to their uniform structure with only few defects, the foams have a high compressive strength. The high strength is also caused by the presence of intermetallic phases in the cell wall microstructure that, however, make the foams brittle.

Use of pre-alloyed AlMg50 powder as an intrinsic blowing gas source appears as a good strategy to distribute the gas uniformly in the emerging foam and to avoid big pressure differences that damage the structure as it happens for conventional blowing agents. This foaming technique could have the potential to be used in an industrial scale. Further improvements appear possible, e.g. by slightly hydrogenating the AlMg50 powder which would allow reducing its content and would help making the foams more ductile.

Received: ((will be filled in by the editorial staff))
Revised: ((will be filled in by the editorial staff))
Published online: ((will be filled in by the editorial staff))

- [1] J. L. Grenestedt, *J. Mech. Phys. Sol.* **1998**, *46*, 29.
- [2] J. L. Grenestedt, K. Tanaka, *Scripta Mater.* **1999**, *40*, 71.
- [3] E. W. Andrews, G. Gioux, P. Onck, L. J. Gibson, *Int. J. Mech. Sci.* **2001**, *43*, 701.
- [4] L. Helfen, T. Baumbach, H. Stanzick, J. Banhart, A. Elmoutaouakkil, P. Cloetens, *Adv. Eng. Mater.* **2002**, *4*, 808.
- [5] B. Matijasevic-Lux, J. Banhart, S. Fiechter, O. Görke, N. Wanderka, *Acta Mater.* **2006**, *54*, 1887.
- [6] M. Mukherjee, *Evolution of Metal Foams during Solidification*, Ph.D. Thesis, TU Berlin, **2009**.
- [7] M. Mukherjee, F. Garcia-Moreno, J. Banhart, *in preparation*.
- [8] M. Mukherjee, C. Jimenez, F. Garcia-Moreno, J. Banhart, German Patent Application DE 10 2009 020 004.5, **2009**.
- [9] H. -M. Helwig, S. Hiller, F. Garcia-Moreno, J. Banhart, *Metal. Mater. Trans. B*, **2009**, *40B*, 755.
- [10] C. Jimenez, F. Garcia-Moreno, J. Banhart, G. Zehl, in *Porous Metals and Metallic Foams* (Eds: L. P. Lefebvre, J. Banhart, D. Dunand), DEStech Publications, Pennsylvania, **2008**, 59.
- [11] N. A. Belov, D. G. Eskin, A. A. Aksenov, *Multicomponent Phase Diagrams: Applications for Commercial Aluminum Alloys*, Elsevier, Oxford, **2005**, 87.
- [12] P. Villars, A. Prince, H. Okamoto, *Handbook of Ternary Alloy Phase Diagrams*, ASM International, Materials Park, OH, **1995**, 3938.
- [13] F. Garcia-Moreno, N. Babcsan, J. Banhart, *Coll. Surf. A*, **2005**, *263*, 290.
- [14] F. Garcia-Moreno, M. Fromme, J. Banhart, *Adv. Eng. Mater.* **2004**, *6*, 416.

- [15] A. Andreasen, M. B. Sørensen, R. Burkarl, B. Møller, A. M. Molenbroek, A. S. Pedersen, J. W. Andreasen, M. M. Nielsen, T. R. Jensen, *J. Alloy. Compd.* **2005**, 404–406, 323.
- [16] A. S. Palma, J. L. Iturbe-García, B. E. López-Muñoz, A. S. Jiménez, *Int. J. Hydrog. Energy.* **2009**, doi:10.1016/j.ijhydene.2009.09.073.
- [17] C. D. S. Tuck, in *Hydrogen Effects in Materials* (Eds. I. M. Bernstein, A. W. Thomson), The Metallurgical Society of AIME, Warrendale, **1981**, 503.
- [18] L. Rokhlin, in *Landolt-Börnstein New Series IV/11A3 – Ternary Alloy Systems* (Eds: G. Effenberg, S. Ilyenko), Springer Berlin Heidelberg, Berlin, **2005**, 64.
- [19] G. M. Scamans, *J. Mater. Sci.* **1978**, 13, 27.
- [20] R. G. Song, W. Dietzel, B. J. Zhang, W. J. Liu, M. K. Tseng, A. Atrens, *Acta Mater.* **2004**, 52, 4727.
- [21] J. Banhart, J. Baumeister, M. Weber, in *European Conference on Advanced PM Materials*, EPMA, Shrewsbury, **1995**, 201.
- [22] D. Lehmhus, J. Banhart, *Mater. Sci. Eng. A*, **2003**, 349, 98.
- [23] E. Koza, M. Leonowicz, S. Wojciechowski, F. Simancik, *Mater. Lett.* **2003**, 58, 132.
- [24] D. Lehmhus, G. Rausch, *Adv. Eng. Mater.* **2004**, 6, 313.
- [25] D. Lehmhus, M. Busse, *Adv. Eng. Mater.* **2004**, 6, 391.
- [26] J. Kovacik, F. Simancik, *Met. Mater.* **2004**, 42, 79.
- [27] A. R. Kennedy, S. Asavavisithchai, *Adv. Eng. Mater.* **2004**, 6, 400.
- [28] K. Stöbener, M. Weigend, G. Rausch, in *Cellular Metals: Manufacture, Properties, Applications* (Eds: J. Banhart, N. A. Fleck, A. Mortensen), MIT-Verlag, Birlin, **2003**, 161.
- [29] A. Chethan, *Zinc Foam: Stabilisation and Characterisation*, Masters Thesis, IIT Madras, **2007**.
- [30] A. R. Kennedy, *Scripta Mater.* **2002**, 47, 763.

- [31] F. von Zeppelin, M. Hirscher, H. Stanzick, J. Banhart, *Compos. Sci. Tech.* **2003**, *63*, 2293.
- [32] C. Körner, M. Arnold, R. F. Singer, *Mater. Sci. Eng. A*, **2005**, *396*, 28.
- [33] V. Gergely, B. Clyne, *Adv. Eng. Mater.* **2000**, *2*, 175.
- [34] M. F. Ashby, A. G. Evans, N. A. Fleck, L. J. Gibson, J. W. Hutchinson, H. N. G. Wadley, *Metal Foams: A Design Guide*, Butterworth-Heinemann, Boston, **2000**, 49.
- [35] J. Banhart, J. Baumeister, *J. Mater. Sci.* **1998**, *33*, 1431.

Fig. 1. Area expansion and temperature profile as a function of time for (a) Al- and (b) Zn-based alloy foams.

Fig. 2. Optical micrographs of (a) AlMg15Cu10, (b) AlMg26Cu10, (c) ZnAl3.3Mg3.3 and (d) ZnAl5.2Mg5.2 foam. Each micrograph corresponds to the foam that shows maximum expansion in Fig. 1.

Fig. 3. 3D cell size distribution in AlMg15Cu10 foam. The volume contribution by each type of cells in the total volume of the foam is written as $\frac{N_i \times V(D_i)}{\sum N_i \times V(D_i)} \times 100\%$. Here N_i is the number of cells having D_i equivalent diameter, and $V(D_i)$ is the volume of cell with D_i diameter. The distribution is fitted with a Gaussian distribution curve. The mean diameter (D) and standard deviation (σ) are given. Inset: 3D tomography reconstruction of the analysed part of the foam showing a volume of about $19 \times 13.3 \times 28.4 \text{ mm}^3$. The calculated porosity is 73.4%.

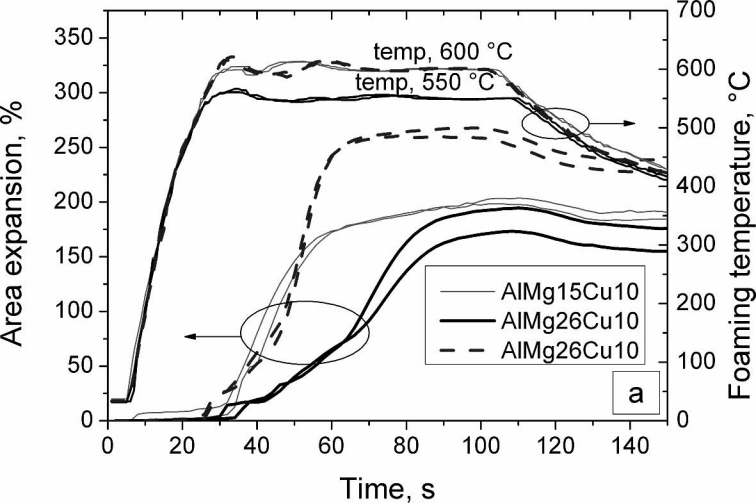
Fig. 4. Stress-strain behaviour of AlMg15Cu10 foam under quasi-static compression. The density of the foam is 0.72 g.cm^{-3} .

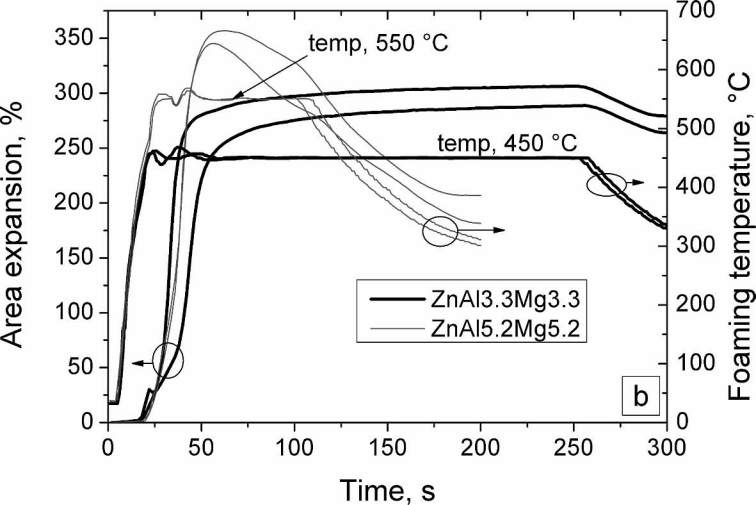
Fig. 5. Schematic view of hydrogen gas flux a) from TiH_2 particles (filled ellipses) contained in conventional foamable precursor, b) from the hydrogen sources in precursors containing AlMg50. Arrows indicate hydrogen flux. Thick arrows suggest stronger flux along grain boundaries.

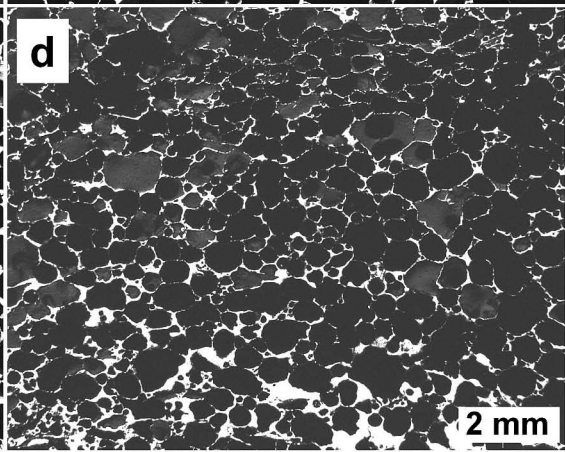
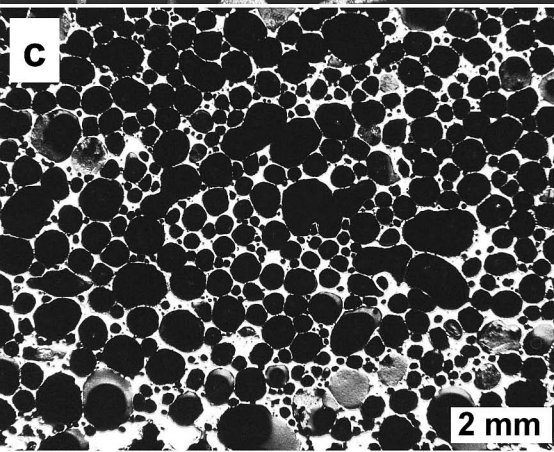
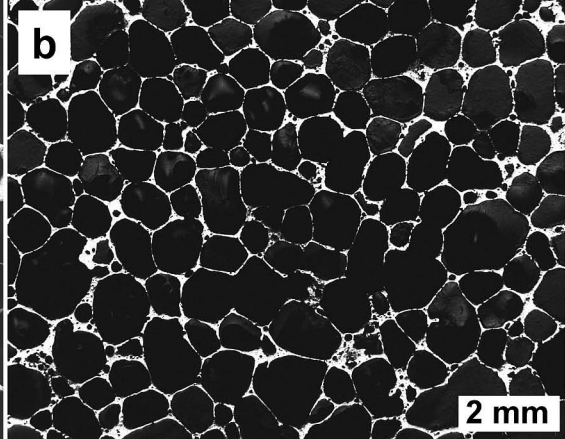
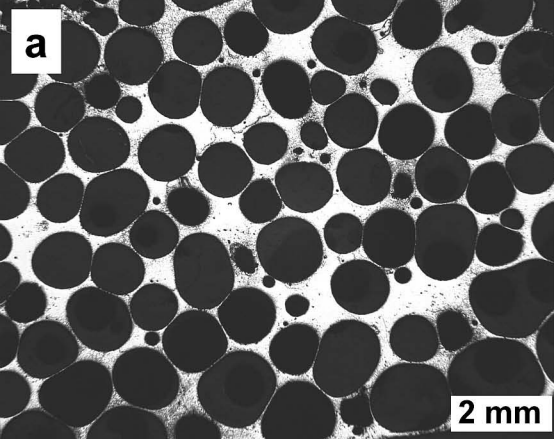
Table 1. Alloy composition, compaction temperature, melting range and expansions

[a] Approximate values according to phase diagram, [b] Measured by AXIM assuming circular symmetry around foaming axis, [c] derived from the volume expansion as measured by AXIM

Sample	Compaction Temperature (°C)	Melting range (°C)[a]	Volume expansion (%) [b]		Relative density of solid foam (%) [c]
			Maximum in liquid state	After solidification	
AlMg15Cu10	400	450–560 ^[11]	248	229	30.4
AlMg26Cu10	350	450–480 ^[11]	311	265	27.4
ZnAl3.3Mg3.3	300	340 ^[12]	332	288	25.8
ZnAl5.2Mg5.2	300	340–420 ^[12]	483	256	28.1





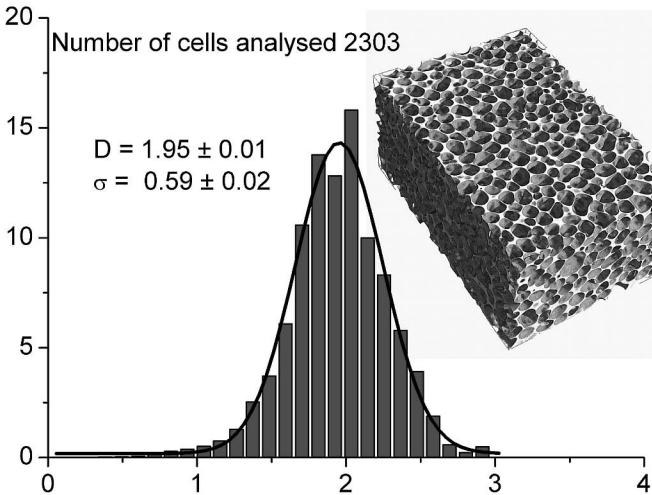


Number of cells analysed 2303

$$D = 1.95 \pm 0.01$$

$$\sigma = 0.59 \pm 0.02$$

Volume contribution, %



Equivalent diameter, mm

